J. Chem. Sci., Vol. 122, No. 6, November 2010, pp. 847–855.

Blue and white light electroluminescence in a multilayer OLED using a new aluminium complex

PABITRA K NAYAK[1], NEERAJ AGARWAL[1,3], FARMAN ALI[1], MEGHAN P PATANKAR[2], K L NARASIMHAN[2,*] and N PERIASAMY[1,*]

[1]Department of Chemical Sciences, [2]Department of Condensed Matter Physics and Materials Science, Tata Institute of Fundamental Research, Homi Bhabha Road, Colaba, Mumbai 400 005

[3]Centre for Excellence in Basic Sciences, University of Mumbai Kalina Campus, Santa Cruz (E), Mumbai 400 098

e-mail: peri@tifr.res.in; kln@tifr.res.in

MS received 21 May 2010; revised 22 July 2010; accepted 19 August 2010

Abstract. Synthesis, structure, optical absorption, emission and electroluminescence properties of a new blue emitting Al complex, namely, *bis*-(2-amino-8-hydroxyquinolinato), acetylacetonato Al(III) are reported. Multilayer OLED using the Al complex showed blue emission at 465 nm, maximum brightness of ~425 cd/m^2 and maximum current efficiency of 0·16 cd/A. Another multilayer OLED using the Al complex doped with phosphorescent Ir complex showed 'white' light emission, CIE coordinate (0·41, 0·35), maximum brightness of ~970 cd/m^2 and maximum current efficiency of 0·53 cd/A.

Keywords. Alq_3; photoluminescence; electroluminescence; blue OLED; WOLED; DFT.

1. Introduction

Development of new electroluminescent organic materials is an active area of research[1–4] and a large effort is under way to make organic light emitting device (OLED)-based technology to develop blue electroluminescence for full colour displays and white light illuminant applications.[5–7] Performance of blue emitting OLEDs is not as efficient as that of green or red and the main problems are their colour purity, stability and lifetime and hence the search for new molecules for blue electroluminescence (EL). Among the best performing light emitting materials, *tris*(8-hydroxyquinolinato) Al(III), (Alq_3) has been used widely because of its strong green emission at ~515 nm, ability to act as electron transport material as well as host material for several phosphorescent dopants.[8] It is known that substitution of electron withdrawing/donating functional groups in specific position in the ligand, 8-hydroxyquinoline, would change the emission property of the Al complex. In Alq_3, the HOMO of 8-hyrdoxyquinoline is mainly over the ring containing oxygen and the LUMO is on the part of the ring that contains nitrogen[9] (also see supporting information). There are two possible ways to increase the HOMO–LUMO gap of the molecule – by attaching an electron withdrawing group in the O-ring at 5 and 7 positions or an electron donating group in the N-ring at 2 or 4 position. There have been numerous attempts to design the structure of an aluminium complex of 8-hydroxyquinoline derivative as ligand with blue photoluminescence (PL) emission.[9–13] Tuning the energy levels by attaching various substituents in the 5 position was carried out and the emission spectrum shifted significantly, but the shortest wavelength attained thereby was 479 nm.[9,13]

Theoretical calculations indicated that a larger blue shift in PL is possible for an Al complex of 8-hydroxyquinoline with an electron donating group (NH_2) at 2 position. In this paper, we report that blue shift of PL and EL maximum to 465 nm is achieved for a mixed ligand, Al complex of 2-amino-8-hydroxyquinoline. Synthesis, photophysical, electrochemical, PL and EL properties, including blue and white light EL, of *bis*-(2-amino-8-hydroxyquinolinato), acetylacetonato Al(III) are described.

*For correspondence

2. Experimental

2.1 *Materials and methods*

2,3,5,6-tetrafluoro-7,7′,8,8′-tetracyano-*p*-quinodimethane (F_4TCNQ) was purchased from Lumetech (Taiwan). 8-hydroxyquinoline, N-N′-diphenyl-N,N′-(*bis*(3-methylphenyl)-1,1′-biphenyl-4,4′-diamine (TPD) and 4,7-diphenyl-1,10-phenanthroline (BCP) were purchased from Sigma-Aldrich (USA) and were used as received. All the solvents were obtained from SD Fine Chemicals (India). ^{1}H and ^{13}C NMR spectra were recorded using Bruker NMR spectrometer (AVANCE WB 500), with working frequency 500 MHz for ^{1}H NMR and 125 MHz for ^{13}C NMR. XRD and crystal structure data were obtained using Nonius MACH3 (IIT Mumbai). Cyclic voltammetry experiments were done with CH Instrument 600 (USA). Absorption spectra of molecules in solution and as thin film were recorded on UV/Vis spectrophotometer (Lambda 25, Perkin Elmer). Steady state fluorescence spectra were recorded using a spectrofluorimeter (SPEX model 1681T). Time resolved fluorescence decays were obtained by the time correlated single photon counting method.[14,15] OLED devices were fabricated on pre-patterned, pre-cleaned ITO-coated glass substrates. The substrates were patterned using standard lithography and then cleaned by mechanical scrubbing with detergent, followed by ultrasonic cleaning in hot water and finally blow drying using dry N_2 gas. The patterned ITO substrate is UV exposed for 10 min. Organic and metal layers were then deposited by thermal evaporation in a high-vacuum ($\sim 10^{-6}$ torr) chamber. A thick layer of LiF (100 nm) was deposited on top of Al cathode to act like a capping layer. The thickness of various layers was monitored using a quartz crystal thickness monitor.

The current, voltage and EL intensity characteristics of the devices were measured in vacuum using a Keithley 617 programmable electrometer. EL measurement was done with a calibrated silicon photodiode. EL spectra were recorded using a monochromator and photomultiplier Tube (S-20 response) operated at 720 V. The EL intensity was converted to cd/m^2 and cd/A using calibrated silicon detector and device and detector geometry. Density Functional Theory (DFT) was used in all the calculations based on the hybrid B3LYP functional using Gaussian03.[16,17]

Synthesis of 2-amino-8-hydroxyquinoline (**3**) by a slightly modified method[18] and the Al complex *bis*-(2-amino-8-hydroxuquinolinaato) acetylacetonato aluminum(III) (**1**) are shown in scheme 1. 8-Hydroxyquinoline was reacted with hydrogen peroxide and acetic acid mixture for three days. Removal of acetic acid followed by extraction and purification by column chromatography produced 8-hydroxyquinoline-N-oxide (**2**) as yellow solid in 38% yield. **2** was reacted with dimethyl sulphate and liquid ammonia to afford **3** in 52% yield. Solutions of **3** (2·0 mmol) and $Al(acac)_3$ (1·0 mmol) in ethanol were mixed and stirred at 60°C. White precipitate of Al complex (**1**) was formed, which was filtered and washed several times with ethanol to remove any soluble impurity, and dried in vacuum to get **1** as white solid in 95% yield. **1** is stable in air and showed high thermal stability. The melting point of **1** was determined by differential thermal analysis to be 321°C. Single crystal of **1** was grown from CH_2Cl_2 and methanol mixture. Figure 1 shows the crystal structure of **1** (see supporting information for details). It can be seen from the structure that two Oxygen atoms of the 2-amino-8-hydroxyquinoline ligand are at the axial position in the structure. It may be noted that **1** crystallizes as one type of isomer though other geometrical isomers are possible in the synthesis. We mention in passing that *tris*(2-amino-8-hydroxyquinolinato) Al(III) could not be synthesized primarily due to steric constraints. Thus, one ligand was replaced by an ancillary non-luminescent ligand, acetyl acetone and **1** was synthesized.

3. Results and discussions

3.1 *Theoretical calculations*

Figure 2 shows the distribution of HOMO and LUMO over the 2-amino-8-hydroxyquinoline ligand in the Al complex **1**. When compared with the distribution over 8-hydroxyquinoline in Alq_3 (see Supporting information) it is seen that the amino group influences the electron density distribution of both HOMO and LUMO of the molecule. The influence on the LUMO is larger than that on the HOMO. This is evident from comparison of quantitative values of ionization potential and electron affinity of **1** and Alq_3. Ionization potential and electron affinity were calculated using DFT at 6-311++G(*d*, *p*) level. In the gas phase, the ionization potential of **1** and Alq_3 are nearly equal, 6·55 eV and 6·63 eV, respectively, suggesting little perturbation of the HOMO level by

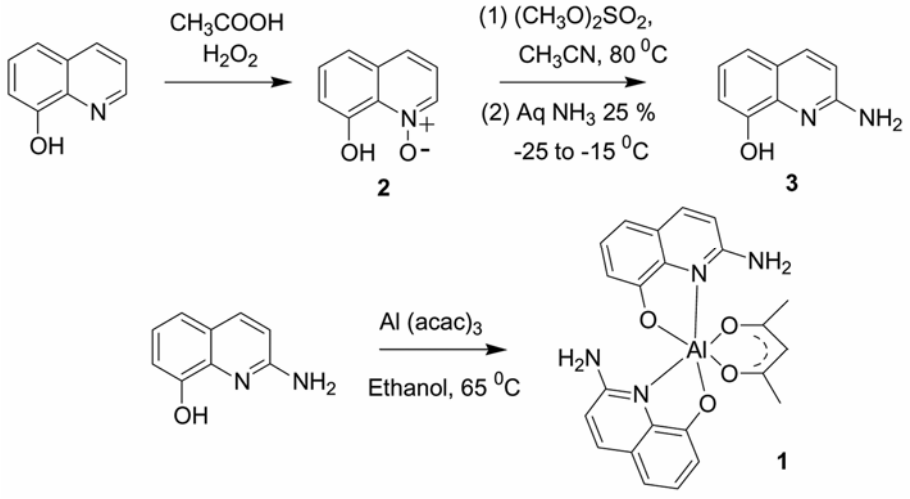

Scheme 1. Synthetic scheme for Al complex **1**.

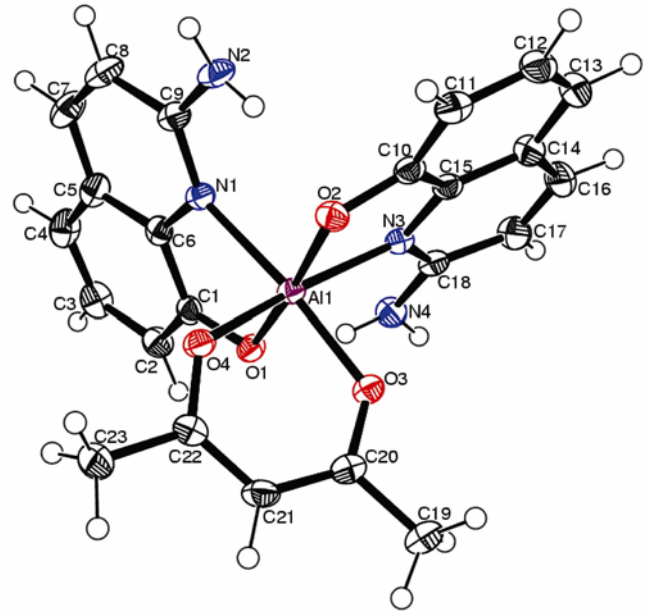

Figure 1. Crystal structure of **1**.

the 2-amino group in **1**. On the other hand, electron affinity of **1** is less at 0·28 eV while that of Alq_3 is 0·91 eV.

Energy levels of molecules in solid state are important in organic electronics. The ionization potential, electron affinity and optical transition energies of **1** and Alq_3 were calculated in solid state using DFT, TD-DFT at 6-311++G(*d*, *p*) level and polarizable continuum model (PCM) by a method reported recently.[19,20] The vertical ionization potential and electron affinity of **1** in the solid state was found to be 5·79 eV and 1·04 eV, respectively. The difference between ionization potential and electron affinity, 4·75 eV is the transport gap. TD-DFT calculation of **1** at 6-311++G(*d*, *p*) level gave the optical band gap of **1** in solid state as 3·23 eV. The corresponding values for Alq_3 in solid state are as follows: ionization potential, electron affinity, transport gap and optical gap are 5·82, 1·66, 4·16 and 2·83 eV, respectively. Thus, the increase in optical gap by 0·4 eV and transport gap by 0·59 eV in **1** is essentially due to decrease of electron affinity due to the 2-amino group. Experimental results are in agreement with the theoretical calculations.

3.2 *Optical absorption and photoluminescence properties*

The absorption spectra of **1** and Alq_3 were recorded in chloroform and are shown in Figure 3. The absorption peak corresponding to π–π^* transition in **1** (~358 nm, molar extinction coefficient is 4076 M^{-1} cm^{-1}) is significantly blue shifted compared to that of Alq_3 (~386 nm). The dilute solution of **1** in chloroform showed emission maximum at 460 nm when excited at the absorption peak, whereas the emission peak of Alq_3 is 516 nm. A smooth thin film of **1** and Alq_3 on quartz were obtained by vacuum deposition and used to record the emission properties in solid state. The emission of **1** in thin film showed peak at 465 nm, a substantial blue shift (~53 nm) of emission maximum compared to Alq_3 (figure 4). The optical gap of **1** in solid state was determined to be 3·08 eV from the intersection of normalized excitation and emission spectra of **1** in thin film. The optical gap for Alq_3 is 2·70 eV.

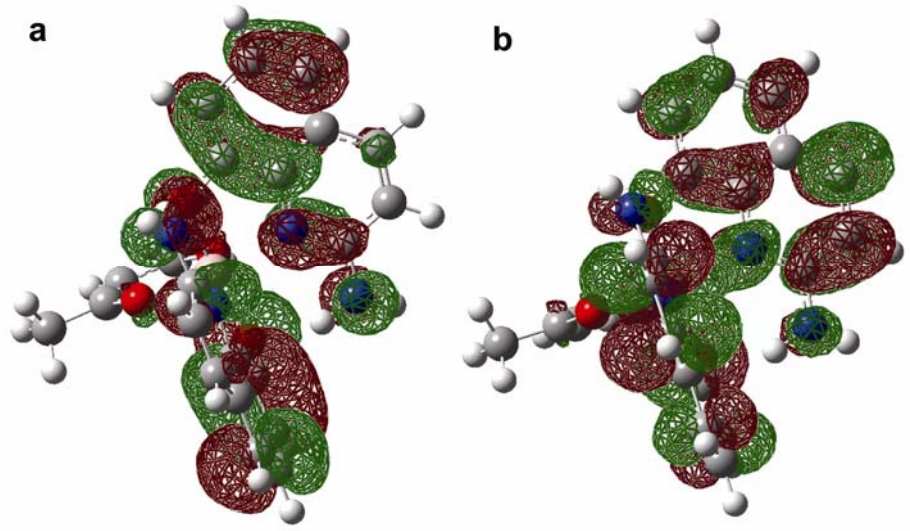

Figure 2. Geometry optimized structure of **1** showing the contribution of (**a**) HOMO and (**b**) LUMO.

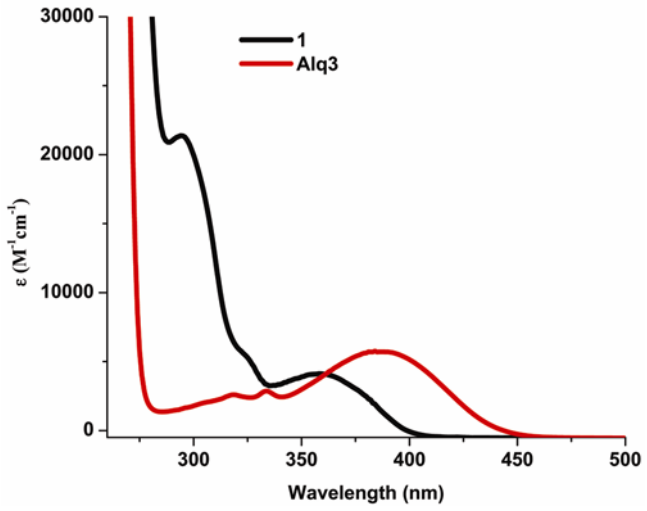

Figure 3. Absorption spectra of Alq_3 and **1** in chloroform.

The PL quantum yield of **1** in chloroform was measured to be 0·08, which is comparable to that of Alq_3 in solution.[21] Absence of self-quenching in Alq_3 in solid film was proven based on PL decay data, and the PL quantum yield is 0·36 in crystalline film.[21] The PL decay of **1** in solution or solid state was biexponential (see supporting information for PL decays and results of analysis), a property that is common with that of Alq_3.[21] Since the material is pure, the origin of biexponential PL decay is either due to intramolecular relaxation and/or intermolecular relaxation (solvent–solute interaction) or heterogeneity (for example, defect sites in solid state). Irrespective of the photophysical origin of biexponential decay, the PL quantum yield is proportional to the area under the PL decay and the average lifetime is a measure of the area under PL decay. The PL quantum yield of **1** in solid state is expected to be same as in solution because of the absence of self quenching indicated by similar average fluorescence lifetime in solution and solid state, which is ~ 1·5 ns.

It is well established that HOMO (ionization potential) and LUMO (electron affinity) energy levels of organic molecules in solid state determined by electron spectroscopy correlate linearly with the cyclic voltammetric oxidation and reduction peak potentials in dichloromethane.[22,23] The shift of redox potential of **1** is thus a measure of shift of HOMO/LUMO level with respect to Alq_3. Cyclic voltammetry of **1** showed irreversible oxidation peak in dichloromethane ([**1**] ~ 1 mM, tetrabutyl ammonium hexafluorophosphate, 0·1 M as supporting electrolyte). The peak potential was observed at 0·58 V with respect to ferrocene. The peak potential for Alq_3 was observed at 0·7 V. The difference in the oxidation potential is 0·12 V whereas the difference is 0·03 eV in ionization potential calculated theoretically. This difference is within the accuracy limit (± 0·15 eV) of theoretical value. **1** was not reducible in the electrochemical range accessible in dichloromethane and therefore it was not possible to compare the corresponding difference in the electron affinity of **1** and Alq_3.

The absolute value of E_{HOMO} of an organic molecule in solid state is important for organic electron-

ics. The usefulness of the electrochemical redox potentials determined in cyclic voltammetry is established.[22,23] However, the value derived thus is only indicative because the polarization energy of the oxidized cation species is expected to be different in solid state and the common polar solvent used in electrochemistry. Nevertheless, a linear relation between E_{HOMO} and V_{ox}, determined using ferrocene (F_c) as internal reference molecule, is established:[22] $E_{HOMO} = -(1{\cdot}4 \pm 0{\cdot}1)\ qV_{ox}$ (vs F_c/F_c^+) $- 4{\cdot}6$ ($\pm 0{\cdot}08$) eV, where q is the electronic charge and V_{ox} is the oxidation peak potential. The cyclic voltammogram of **1** is shown in supporting information. Using the above relation, we obtain E_{HOMO} of **1** as $-5{\cdot}41 \pm 15$ eV. In an alternate method, E_{HOMO} may be placed at 0·58 eV less than that of E_{HOMO} of ferrocene. The latter value may be calculated from the reported oxidation potential of +0·52 V vs Ag/AgCl (ref. 24) in dichloromethane, and therefore +0·72 V vs NHE.[25] The IUPAC recommended value of absolute potential for NHE is $4{\cdot}44 \pm 0{\cdot}02$ eV.[26] Using these data, the E_{HOMO} of ferrocene and **1** are estimated to be –5·16 eV and –5·74 eV, respectively. The value for **1** obtained thus is closer to the theoretically calculated value of 5·79 eV.

The value E_{LUMO} for **1** could not be obtained from electrochemical data. The lower limit for this level is obtained as –2·66 eV by addition of optical band gap energy (3·08 eV) to the E_{HOMO}.

Thus, the experimental values of oxidation potential and optical band gap are consistent with the theoretical values calculated using DFT, TD–DFT and PCM. Table 1 gives a comparison of photophysical properties and energy levels of **1** and Alq_3.

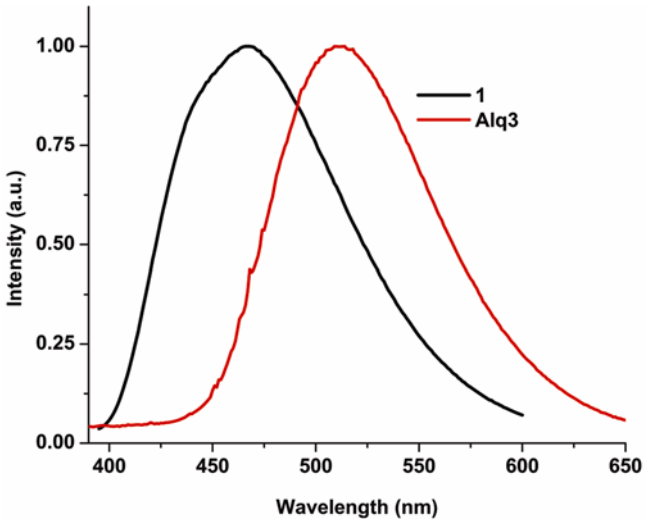

Figure 4. Peak normalized emission spectra of **1** and Alq_3 in solid thin films on quartz.

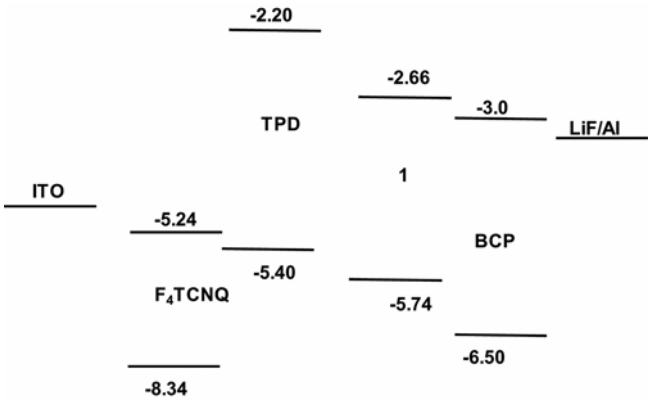

Figure 5. Energy level diagram of molecules.

3.3 *Electroluminescence properties*

The electroluminescence properties (EL) of **1** were studied in the following multilayer OLED structure: ITO/F_4TCNQ(20 Å)/TPD(600 Å)/**1**(600 Å)/BCP(60 Å)/LiF(15 Å)/Al. F_4TCNQ, TPD, **1**, BCP, LiF and Al were successively deposited under high vacuum onto the patterned ITO. The device area was 2 mm^2. The energy levels of all the materials used in the device are shown in figure 5 in the same order as arranged in the device. The HOMO and LUMO levels for F_4TCNQ,[27] TPD (ref. 28) and BCP (ref. 29) are taken from literature. The function of the molecules in each layer as determined by the relative energy levels is as follows. The LUMO level of F_4TCNQ is approximately aligned with that of ITO anode (–4·8 to –5·2 eV) and HOMO level of TPD. Thus, the 20 Å thick F_4TCNQ helps in efficient hole injection from ITO to TPD. BCP serves as an electron transport layer from LiF/Al cathode and also as a hole blocking layer due to the deep HOMO level at –6·50 eV. That is, holes are confined to the doped and undoped layers of **1** as they are blocked by BCP layer to reach cathode. Thus, the device architecture facilitates electron-hole recombination in the doped and undoped layers of **1**.

The device characteristics, namely the plots of current (I) vs voltage (V), EL intensity vs V, EL vs I, and EL efficiency vs I are shown in figures 6A and B. The current and EL turn-on voltages were observed at about 6 V. The sharp rise in the current after turn-on indicates efficient hole and electron injection in the device. Holes are transported by TPD and electron by BCP in the device and electron-hole

Table 1. Peak wavelengths of absorption and emission, fluorescence lifetime and energy levels of **1** and Alq_3.

Compounds	Absorbance peak (nm)	PL peak (nm)[a]	PL peak (nm)[b]	τ (ns)[a]	τ (ns)[b]	Oxidation potential (V vs F_c)	E_{opt} (eV)
Alq_3	386	516	518	16·67[d]	11·43[d]	0·70	2·70[e] 2·83[c]
1	358	460	465	1·46	1·47	0·58	3·08[e] 3·23[c]

[a]In $CHCl_3$, [b]In thin film, [c]Calculated, [d](ref. 21), [e]Experimental

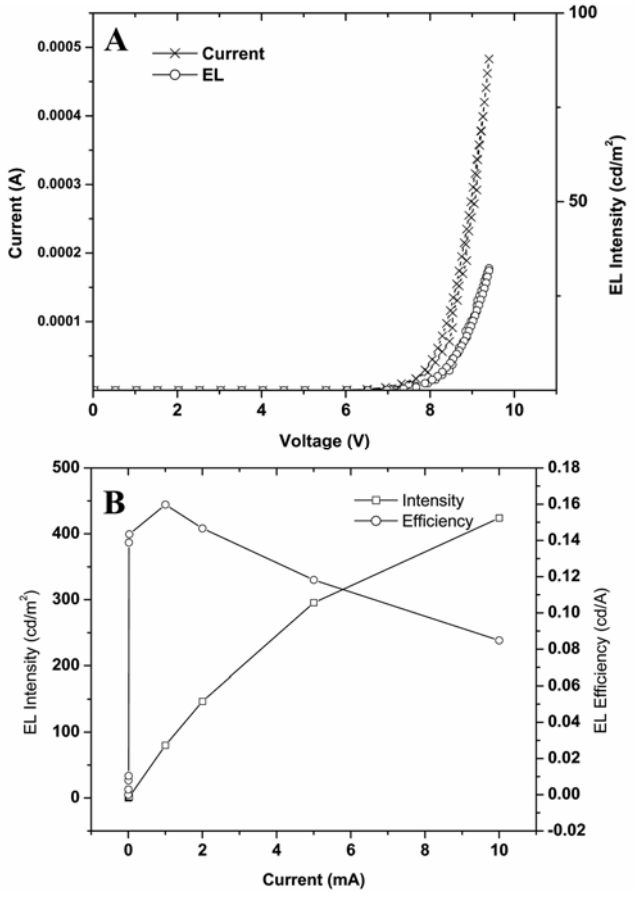

Figure 6. (**A**) Current and EL intensity vs applied voltage for the device (2 mm^2 area) ITO/F_4TCNQ/TPD/**1**/BCP/LiF/Al. (**B**) EL intensity cs current and EL efficiency vs current for the device.

recombination occurs in **1**. The EL spectrum of the blue OLED and PL spectrum of **1** are shown in figure 7. The PL and EL spectra match well and hence the electroluminescence is from **1**. Figure 6A shows that the forward and reverse current-voltage and EL intensity–voltage plots overlapped well upon forward and reverse voltage scans and the hysteresis is negligible. This indicates that trapping of carriers (hole or electron) in the organic layers is negligible in this device. The current efficiency (cd/A) of the OLED was calculated as the ratio of EL intensity (cd/m^2) and current density (A/m^2). The current efficiency vs current and EL intensity vs current plots are shown in Figure 6B. It is seen that the EL intensity is not saturated at the maximum current or current density and further improvement in performance is possible. The maximum current efficiency is 0·16 cd/A at 80 cd/m^2 which declines to 0·08 cd/A at 425 cd/m^2. The CIE coordinates for the blue EL were calculated to be 0·19, 0·23. To our knowledge, the blue OLED with EL peak at 465 nm reported here is the shortest wavelength, blue emitting OLED using an Alq_3-type molecule reported so far.

3.4 *Near white light device using* **1** *and an iridium complex*

The blue OLED described above using **1** has the potential to generate other colours of lower photon energy or white light by addition of dopant molecules in or adjacent to the emitting layer. The applications of a variety of heteroleptic and homoleptic Iridum complexes as dopant molecules in OLED, their synthesis and purification have been reviewed.[30,31] Here we describe a near-white light emitting device (WOLED) using **1** and an orange-red phosphorescent iridium complex, namely, (*bis* [1-(4,6-difluorophenyl)isoquinolinato], acetylacetonato Ir (III)). The structure of the Ir complex is shown in figure 9 (inset). The emissive layer of the white light device consists of two layers, (i) a layer of **1** of thickness 300 Å and (ii) a layer of **1** doped with the Ir complex. These layers were grown under high vacuum sequentially without breaking vacuum. The device structure is ITO/F_4TCNQ (20 Å)/TPD (400 Å)/**1** (300 Å)/[**1** + Ir complex] (300 Å)/BCP (60 Å)/LiF (15 Å)/Al. The [**1** + Ir complex] layer was prepared by co-evaporation of a mixture of **1** and Ir complex in the ratio of 1 : 0·003 mole/mole from the same boat.

The current vs voltage and EL intensity vs voltage plots of the white light OLED are shown in figure 8A. The current efficiency vs current and EL intensity vs current plots are shown in figure 8B. It is seen that the EL intensity is not saturated and further

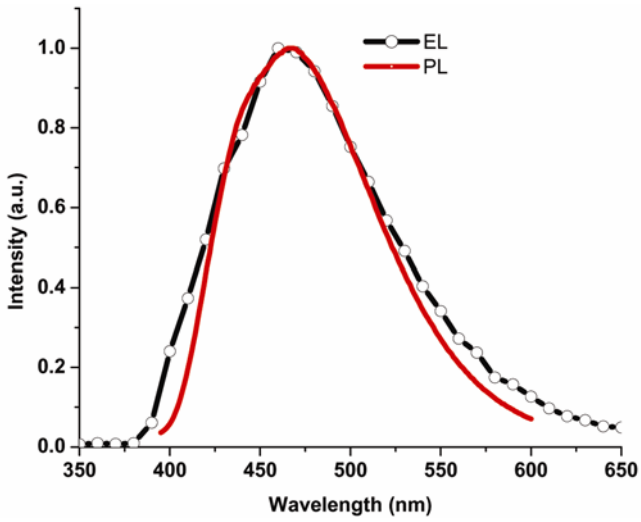

Figure 7. EL spectrum device ITO/F4TCNQ/TPD/**1**/BCP/LiF/Al and PL of **1**.

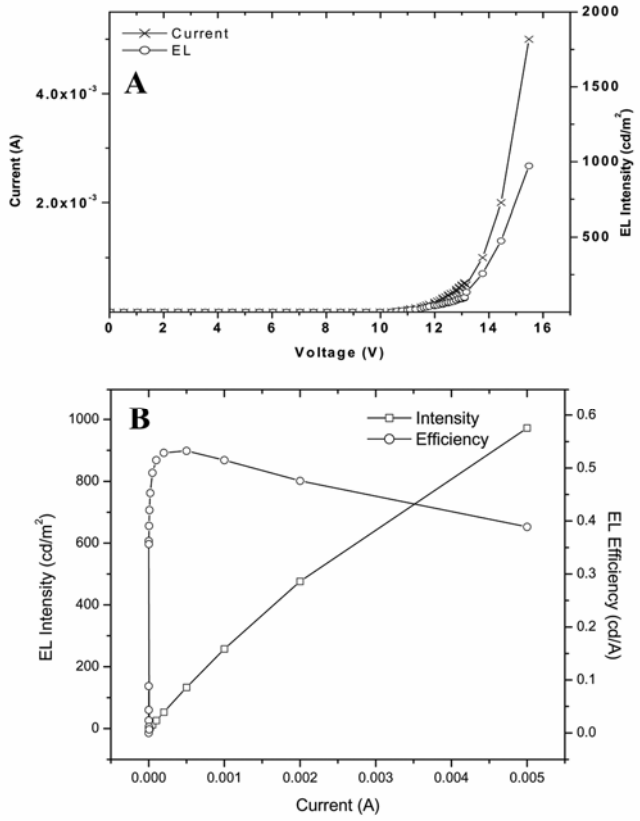

Figure 8. (**A**) Current vs voltage and EL vs voltage diagram for device (2 mm^2 area), ITO/F_4TCNQ/TPD/**1**/[**1** + Ir complex]/BCP/LiF /Al. (**B**). EL intensity vs current and EL efficiency vs current for the same device.

improvement in performance is possible. The maximum current efficiency (cd/A) is 0·53 at ~130 cd/m^2, which declines moderately to 0·39 at ~970 cd/m^2. The EL spectrum of the device is shown in figure 9. The EL spectrum matches well with those of the PL spectra of **1** and Ir complex. It is pertinent to note that the spectrum spans the blue, green and red region of the visible spectrum. The relative EL emission intensity contribution of **1** and Ir complex to the EL spectrum can be adjusted by varying the dopant concentration. For a true white light device the CIE coordinates are 0·33, 0·33. The CIE coordinates for the EL spectrum as shown in figure 9 were calculated to be 0·41, 0·35. The CIE coordinates shift to 0·34, 0·33, very close to true white light, when the intensity contribution of Ir complex is decreased by 50%.

The origin of the EL emission spectra matching with those of **1** and Ir complex may be explained as follows. The energy level diagram for the device is identical to that shown in figure 5 since the mixed layer of **1** is only lightly doped with Ir complex. From the energy levels of the molecules it is expected that the electron-hole recombination zone is near the TPD: **1** interface as well as the layer of **1**, which results in the generation of singlet and triplet excited state of **1** in the ratio of 1 : 3. While the singlet state of **1** emits in blue, the triplet excitons diffuse through the bulk of the 300 Å thick layer of pure **1** to reach the doped layer, where the triplet

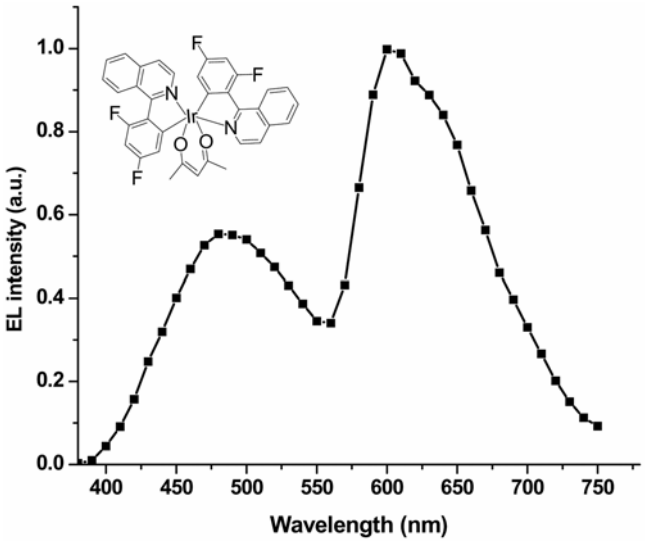

Figure 9. EL spectrum of the device ITO/F_4TCNQ/TPD/**1**/[**1** + Ir complex]/BCP/LiF/Al. Inset shows the structure of Ir complex.

energy is transferred to the Ir complex. The photophysical properties of phosphorescent Ir complexes and their usefulness in OLEDs are recently reviewed.[5] Mainly, the excited state lifetime of luminescent Ir complexes is in microseconds and the quantum yield is very high. Thus, in the context of OLEDs the triplet excitons of **1** are harvested by Ir complex and converted to orange red photons. The EL intensity and current efficiency in Ir doped devices ought to be higher compared to undoped devices. In our case, the maximum current efficiency in doped white light OLED is 0·53 cd/A is three-fold higher compared to the undoped blue OLED (0·16 cd/A), which is along the expected lines.

It is possible that singlet energy of **1** may also be transferred to Ir complex via fluorescence resonance energy transfer (FRET), because of the overlap of absorption spectrum of Ir complex with the emission spectrum of **1**. In order to retain the blue emission of **1,** the FRET process shall have to be prevented. This is achieved by separating the pure layer of **1** from the doped layer. Moreover, 300 Å thickness is rarer than the diffusion length of singlet exciton of nanosecond lifetime. Thus, this architecture of the device produces emission from both singlet (blue) of the Al complex and triplet (orange-red) of Ir complex.

4. Conclusions

A new blue emitting Al complex, *bis*-(2-amino-8-quinolinolato), acetylacetonato Al(III) was synthesized and its photophysical, elctrochemical and energy level properties were studied and compared with *tris*(8-hydroxyquinolato) Al(III). We have demonstrated blue EL using this molecule. We have also demonstrated a white light OLED using the Al complex by incorporation of an additional layer doped with an orange-red emitting Iridium complex. The maximum brightness and maximum current efficiency of the blue and white OLEDs were 425 cd/m^2 and 0·16 cd/A, and ~970 cd/m^2 and 0·53 cd/A, respectively.

Supporting information

HOMO and LUMO distribution in Alq_3, ^{1}H NMR spectrum of **1**, cyclic voltammogram, emission and excitation spectra in solid state, PL decays and crystallographic data of **1** are provided (see www.ias.ac.in/chemsci).

References

1. Shinar J 2003 *Organic light-emitting devices* (New York: Springer-Verlag)
2. Li Z and Meng H (eds) 2007 *Organic light-emitting materials and devices* (New York: CRC Taylor and Francis)
3. Miller R D and Chandross E A 2010 *Chem. Rev.* **110** 1
4. Koch N 2007 *Chem. Phys. Chem.* **8** 1438
5. Baranoff E, Yum J, Graetzel, M and Nazeeruddin Md K 2009 *J. Organometal. Chem.* **694** 2661
6. Roncali J, Leriche P and Cravino A 2007 *Adv. Mater* **19** 2045
7. Anzenbacher Jr. P, Montes, V A and Takizawa S 2008 *Appl. Phys. Lett.* **93** 163302
8. Baldo M A, O'Brien D. F. You Y, Shoustikov A, Sibley S, Thompson M E and Forrest S R 1998 *Nature* **395** 15
9. Burrows P E, Shen Z, Bulovic V, McCarty D M, Forrest S R, Cronin J A and Thompson M E 1996 *J. Appl. Phys.* **79** 7991
10. Montes V A, Li R G, Shinar J and Anzenbacher Jr P 2004 *Adv. Mater.* **16** 2001
11. Montes V A, Pohl R, Shinar J and Anzenbacher Jr P 2006 *Chem. Eur. J.* **12** 4523
12. Perez-Bolıvar C, Montes V A and Anzenbacher Jr P 2006 *Inorg. Chem.* **45** 9610
13. Hopkins T A, Meerholz K, Shaheen S, Anderson M L, Schmidt A, Kippelen B, Padias A B, Hall H K, Peyghambarian N and Armstrong N R 1996 *Chem. Mater.* **8** 344
14. O'Connor D V and Phillips D 1984 *Time correlated single photon counting* (London: Academic Press)
15. Periasamy N, Maiya B G, Doraiswamy S and Venkataraman B 1988 *J. Chem. Phys.* **88** 1638
16. Frisch M J *et al* 2004 Gaussian 03, revision C.02; Gaussian, Inc. Wallingford, CT
17. Cramer C J 2003 *Essentials of computational chemistry* (England: Wiley)
18. Storz T 2004 *Organic Proc. Res. and Develop.* **8** 663
19. Nayak P K and Periasamy N 2009 *Organ. Electron.* **10** 532
20. Nayak P K and Periasamy N 2009 *Organ. Electron.* **10** 1396
21. Ravi Kishore V V N, Narasimhan K L and Periasamy N 2003 *Phys. Chem. Chem. Phys.* **5** 1386
22. D'Andrade B W, Datta S, Forrest S R, Djurovich P, Polikarpov E and Thompson M E 2005 *Org. Electron.* **6** 11
23. Djurovich P, Mayo E I, Forrest S R and Thompson M E 2009 *Org. Electron*. **10** 515
24. Noviandri I, Brown K N, Fleming D S, Gulyas, P T, Lay P A, Masters A F and Phillips L 1999 *J. Phys. Chem*. **103** 6713
25. Bard A J and Faulkner L R 2000 *Electrochemical methods: fundamentals and applications* (New York: Wiley) 2nd edn
26. IUPAC, Compendium of Chemical Terminology, 2nd ed. (the 'Gold Book'). Compiled by A. D. McNaught and A. Wilkinson. Blackwell Scientific Publications, Oxford (1997) XML on-line corrected version:

http://goldbook.iupac.org (2006-) created by M. Nic, J. Jirat, B. Kosata; updates compiled by A. Jenkins. ISBN 0-9678550-9-8. doi:10.1351/goldbook
27. Gao W and Kahn A 2002 *Organ. Electron.* **3** 53
28. Mishra A, Nayak P K, Ray D, Patankar M P, Narasimhan K L and Periasamy N 2006 *Tett. Lett*. **47** 4715
29. Rand B P, Li J, Xue J, Holmes R J, Thompson M E and Forrest S R 2005 *Adv. Mater.* **17** 2714
30. Baranoff E, Yum J H, Graetzel M and Nazeeruddin Md K J 2009 *Organometal. Chem.* **694** 2661
31. Lamansky S, Djurovich P, Murphy D, Abdel-Razzaq F, Kwong F R, Tsyba I, Bortz M, Mui B, Bau R and Thompson M E 2001 *Inorg. Chem.* **40** 1704